N90-27572

C I, C II, AND CO AS TRACERS OF GAS PHASE CARBON

Jocelyn Keene
California Institute of Technology

In this talk I will be discussing the form of gas phase carbon in the dense interstellar medium. Since this is a very mixed audience, I will make this talk more of a tutorial, using illustrative references only, than a comprehensive review. Some relevant questions for this discussion are:

1. What are the major forms of gas phase carbon in the dense interstellar medium?
2. What are their abundances relative to hydrogen?
3. How are the major components related?
4. What controls their relative abundances and distribution?

I will try to answer the first two of these questions and will only briefly touch on the last two.

The discussion will center on dense molecular clouds for two reasons: *a*) molecular clouds are the sites of most of the interesting chemical processes in the interstellar medium and *b*) gaseous carbon in the diffuse interstellar medium is thought to be almost entirely singly ionized. Typical molecular clouds have kinetic temperatures of 10–100 K, depending on whether they are associated with star-formation regions. Average densities for giant molecular clouds are $n(H_2) \gtrsim 10^2$ cm^{-3}, but this discussion will be slanted toward smaller and denser condensations, $n(H_2) \gtrsim 10^4$ cm^{-3}, often associated with star formation.

It is thought that molecular clouds contain approximately half of the Galaxy's total gaseous mass although they occupy only a small fraction of the volume of the Galaxy. The imbalance between mass and volume occurs because, except for dense self-gravitating clouds, the general interstellar medium is approximately in pressure equilibrium and the other gas phases have higher temperatures and lower densities. Another small volume is occupied by cool neutral atomic gas, $T \lesssim 100$, concentrated in structures called "diffuse clouds" which may be associated with molecular clouds. About half of the volume of the Galaxy is occupied by neutral atomic and ionized gas components with temperatures $T \lesssim 8000$K and rest of it is occupied by a very hot, $T \sim 10^6$ K, highly ionized gas component.[1]

FUNDAMENTAL DATA

Table 1 is a list of the most abundant elements, with their ionization potentials.[2] It is important to notice three things:

1. carbon is the fourth most abundant element in the universe, with an abundance relative to hydrogen of 3.3×10^{-4}.
2. carbon's ionization potential, 11.26 eV, is the only one of the first 6 elements in this table lower than that of hydrogen. Not until iron, which is a factor of 8 less abundant, do you find a lower ionization potential. This means that, among atoms, carbon has virtually no competition for the interstellar ultraviolet radiation with photon energy between 11.26 and 13.6 eV and it will be easily ionized unless it is shielded by dust, an efficient continuum absorber of radiation.
3. the dissociation potential for the carbon monoxide molecule, listed at the bottom of the table, is very close to the ionization potential for carbon. Carbon monoxide is a very stable molecule, not highly reactive. In a shielded environment in which chemical reactions can occur it is the endpoint of these reactions. Also, oxygen, which is the other component of carbon monoxide, is twice as abundant as carbon. Therefore in a shielded environment it would be reasonable to expect most of the carbon to be in the form of CO.

TABLE 1

COSMIC ABUNDANCES

Element	Abundance	Ionization Potential (eV)
H	1.0	13.60
He	8.5×10^{-2}	24.59
O	6.6×10^{-4}	13.62
C	3.3×10^{-4}	11.26
N	9.1×10^{-5}	14.53
Ne	8.3×10^{-5}	21.56
Fe	4.0×10^{-5}	7.87
Si	3.3×10^{-5}	8.15
Mg	2.6×10^{-5}	7.65
S	1.6×10^{-5}	10.36
Molecule		**Dissociation Potential (eV)**
CO		11.09

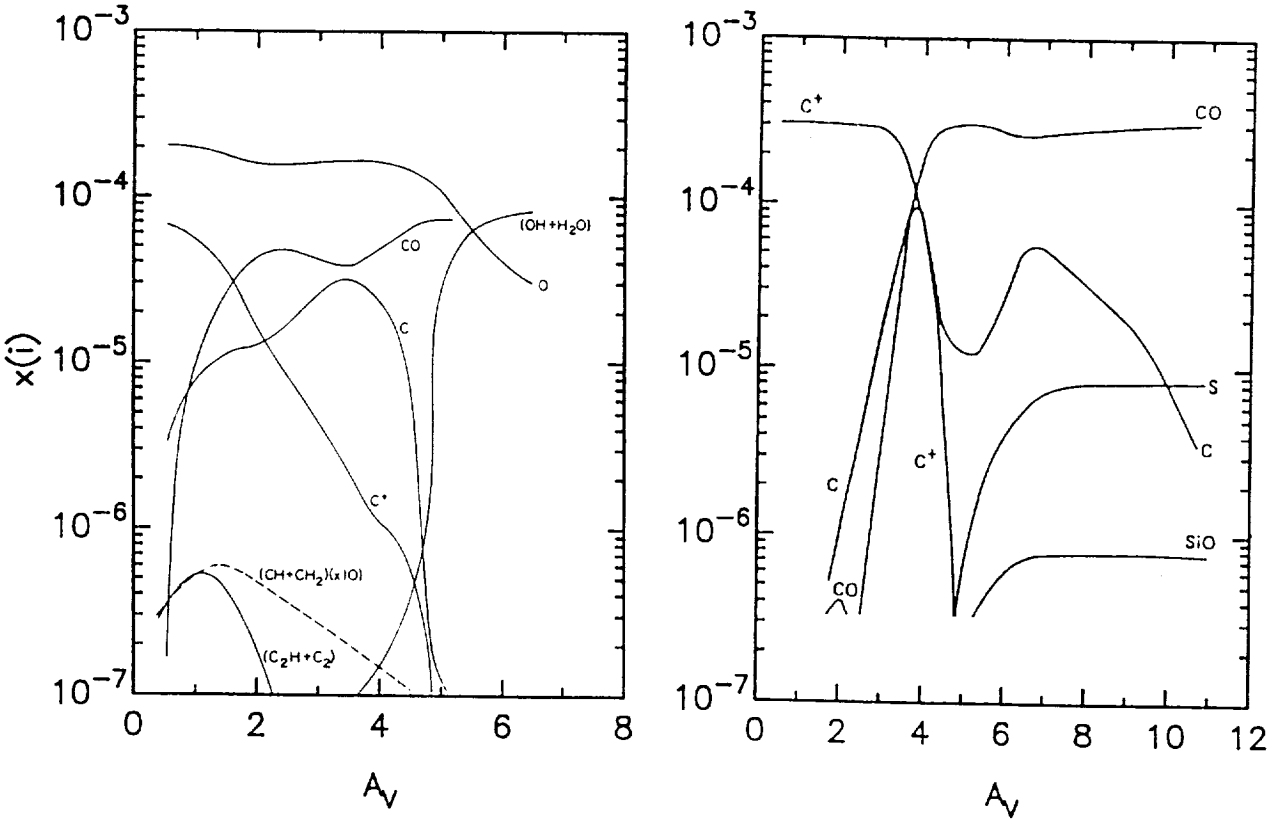

FIG. 1. – Fractional abundances as a function of visual extinction into a cloud *left*) from Langer,[3] with $T = 20$ K, $n(H) = 10^3$ cm^{-3}, $G = G_o$; *right*) from Tielens and Hollenbach,[4] with $T = T(A_V)$, $n(H) = 2.3 \times 10^5$ cm^{-3}, $G = 10^5\ G_o$.

RESULTS OF CALCULATIONS

Steady state calculations, including the effects of the ultraviolet radiation field and chemical reactions, show that one might expect most of the carbon outside dense clouds to be ionized (hereafter C II), most of it within dark clouds to be in the form of carbon monoxide (CO), and, at the edges of clouds between these two regions, a fraction of it to be in a thin layer of neutral atomic carbon (C I). All other gas phase forms of carbon should be negligible compared with these. Figure 1 shows the results of two calculations on the abundances of carbon species near the edge of a cloud under different sets of conditions: *left*) a calculation for the case of a cool (20 K) cloud immersed in the general interstellar radiation field, and *right*) the Orion Molecular Cloud which lies just behind the Orion Nebula. The ultraviolet field illuminating the cloud (G, measured in units of $G_o = 1.6 \times 10^{-3}$ ergs cm^{-2} s^{-1}, the average intensity of the interstellar field) in the Orion model is enhanced by a factor of 10^5 because of the presence of the hot stars which produce the ionized nebula. Both these calculations show the qualitative results discussed above, i.e., that the carbon is expected to be mostly in the form of C II outside the cloud ($A_V < 1$ to 2) and in the form of CO within the cloud. The exact dividing line between these two regimes and the position of the anticipated narrow shell of C I is determined by the amount of ultraviolet radiation illuminating the cloud.

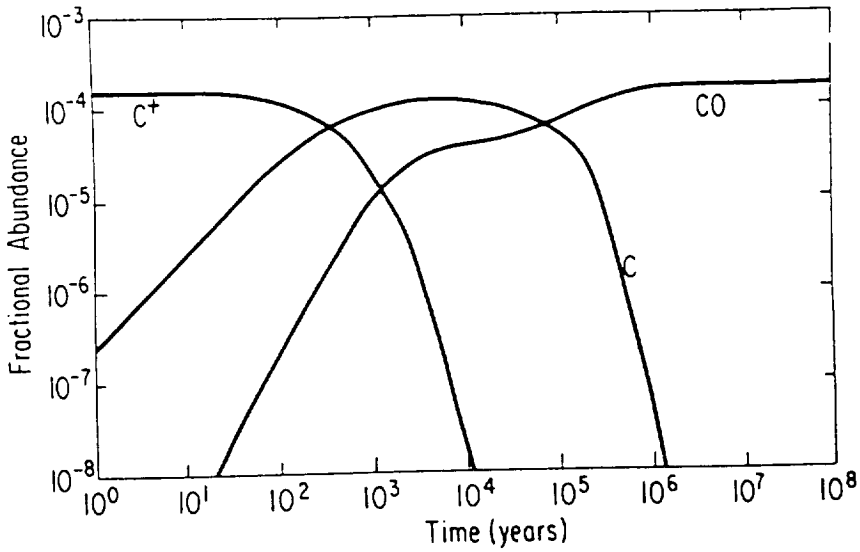

FIG. 2. – Fractional abundances as a function of time at the center of a well shielded cloud of density $n(H_2) = 2 \times 10^4$ cm^{-3} from Leung, Herbst, and Heubner.[5]

Other calculations which follow the chemical time evolution of clouds show analogous effects. Figure 2 shows the results of an evolutionary model which at its origin in time had all the carbon in the form of C II, as a cloud would have before its collapse from the diffuse interstellar medium.[5] Since this calculation did not include the effects of ultraviolet radiation, these results are valid only for a region at the center of a cloud which is completely shielded from the ultraviolet radiation field at the edge. The calculation illustrates the point that $\sim 10^6$ years after the initial collapse of a cloud there should be no C I left in the shielded cloud interiors. Since molecular clouds are thought to exist for at least 10^7 years, shown by the presence of young stars within many of them, the endpoint of this calculation should be relevant for the interiors of most molecular clouds today.

SPECTRA OF CARBON SPECIES

C I, C II, and CO all have transitions in the far-infrared to millimeter wavelength region of the spectrum. This is important because only long wavelengths can pass through the dense material which makes up molecular clouds. They also have transitions in the ultraviolet to infrared spectral region that are useful for studying their abundances

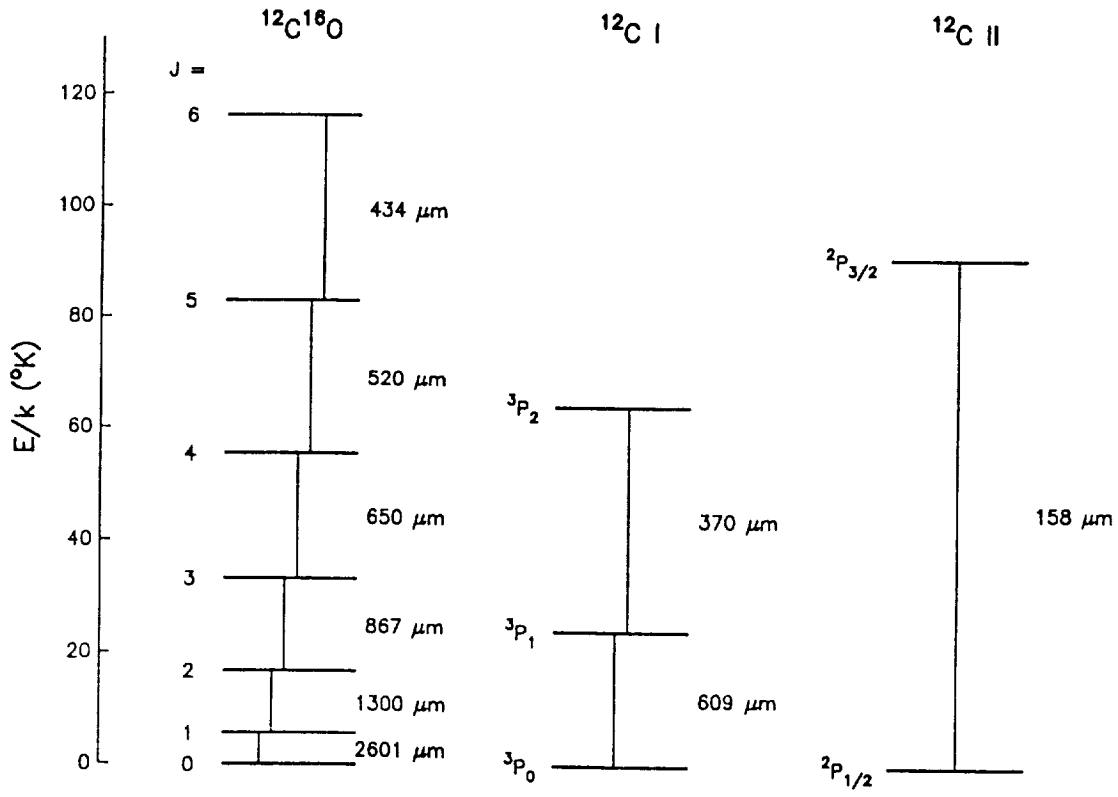

FIG. 3. – Energy levels of the three most common species of gas phase carbon and their transition wavelengths. The lowest transitions of these species all lie in the millimeter to far-infrared wavelength region. The energy levels are appropriate for excitation in typical interstellar clouds ($T \approx 10$–100 K).

in more diffuse matter. Figure 3 shows the low-lying transitions for all three species and the energy of the upper states in units of E/k. The transitions of both C I and C II are magnetic-dipole fine-structure transitions, whereas those of CO are electric-dipole rotational transitions. The C I and CO transitions are well suited to studying both the cold ($T < 20$ K) and the warm ($T > 50$ K) interstellar media because of the presence of energy levels only 10's of degrees above the ground state, as well as higher levels. Unfortunately, the only C II ground state transition is quite high in energy (91 K) and is easily observed only in warm objects.

CO ABUNDANCES

We would like to estimate the abundance of CO relative to hydrogen. This ratio is most often calculated by comparing the line of sight abundance of CO (column density) with the visual extinction (A_V) from dust grains in the same line of sight. It is commonly assumed that the dust to hydrogen mass ratio is constant throughout the Galaxy so the column ratio of CO to hydrogen can be derived.

In order to compute column densities of CO, we have to understand its distribution among the available excitation levels and the photon propagation processes for individual clouds. The lines of the most common form of CO, $^{12}C^{16}O$, are usually optically thick, so that they cannot be used to measure the column density. Luckily both carbon and oxygen have isotopes which, although rare, are observable. In the Solar system the abundance ratios of the main isotopes to the rarer ones are: $^{12}C/^{13}C = 89$, $^{16}O/^{18}O = 500$, and $^{16}O/^{17}O = 2750$.[6] The ratios in the interstellar medium are different from the Solar System values and are a function of position in the Galaxy.[7] Of course the isotopes can also be found in combinations, such as $^{13}C^{18}O$. (Hereafter, I will use the atomic mass superscript only when referring to one of the rare isotopes of carbon or oxygen.) ^{13}CO is usually only moderately optically thick ($\tau \approx 1$ in many sources), and $C^{18}O$ is usually optically thin so that radiative transfer problems are minimized. These, as well as the even rarer forms, can be used to determine the abundance in one of the levels

of the observed transition along a line of sight. One must then correct for both the ratio of the main isotope of CO to the rare species and also for the population which is in other energy levels. One commonly used method for finding the column density of CO, the LTE method, is discussed in the Appendix.

Visual extinction in large areas of clouds is most often measured by the star-counting method in which comparisons of the number of stars in obscured and unobscured regions of sky in the vicinity are used to deduce the amount of extinction.[8,9] Measurements of the ultraviolet H I and H_2 line absorption in the light from hot, bright stars compared with measurements of the visual extinction towards the same stars show that the ratio of hydrogen column density to visual extinction is 1.9×10^{21} atoms cm^{-2}.[10]

RESULTS FROM CO

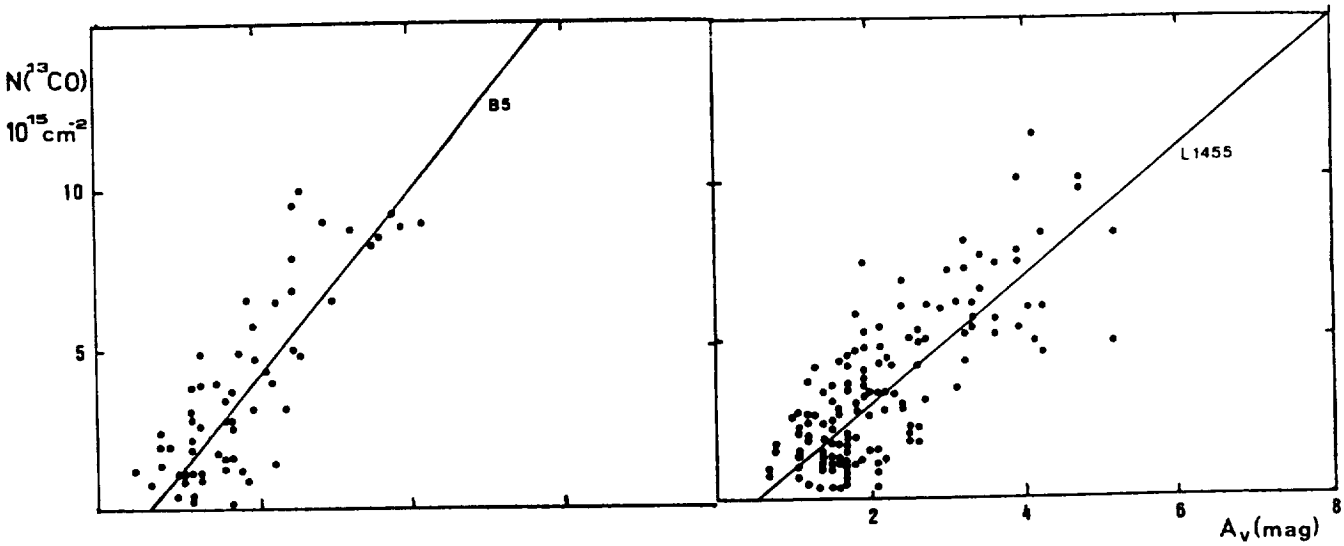

FIG. 4. – The LTE derived column density of ^{13}CO vs A_V in two dark clouds, from Bachiller and Cernicharo.[11]

Figure 4 shows some results for the relation between $N(^{13}CO)$ and A_V in two different molecular clouds. Table 2 contains a summary of many such studies adapted from Bachiller and Cernicharo.[11] Typically the slope of the relation between $N(^{13}CO)$ and A_V is 2×10^{15}. Since $N(CO)/N(^{13}CO) \approx 60$ in the solar neighborhood[7] and since $N(H + 2H_2)/A_V \approx 1.9 \times 10^{21}$ atoms cm^{-2}, the ratio between CO and total hydrogen abundance is approximately 6.3×10^{-5}. It is possible to use observations of $C^{18}O$ rather than ^{13}CO; the results are similar. Referring back to Table 1 we see that this implies that within molecular clouds about 20% of the carbon is in the form of CO.

PROBLEMS WITH CO

There are several problems associated with deriving the ratio of CO column density to H_2 via visual extinction.

1. The ratio of H I plus H_2 column density to visual extinction has been measured only in lines of sight with less than 2 mag of extinction.[10] Even at such low extinctions some clouds have a law for extinction as a function of wavelength that is different from that of the average. The implications of this are that such clouds, for example the one near the star ρ Ophiuchi, contain dust grains which differ from grains in more diffuse clouds, most probably in the grain size distribution. For the same total mass of dust, a cloud which has large dust grains will have less extinction than one with small grains. This means that $N(H + 2H_2)/A_V$ may vary from cloud to cloud and even from center to edge of the same cloud.
2. Over large areas of sky only small values of visual extinction can be measured reliably. At positions of large extinction no background stars are visible and thus the extinction is not measurable. For this reason,

TABLE 2

RELATION BETWEEN CO ABUNDANCE AND A_V

Cloud	$N(^{13}CO)$ (cm^{-2})	$N(C^{18}O)$ (cm^{-2})	Comments	Reference
ρ Oph	$2.5 \times 10^{15} A_V$			14
L134	$3.8 \times 10^{15} A_V$			15
many	$2.0 \times 10^{15} A_V$			16
L43	$1.5 \times 10^{15} A_V$			17
Taurus	$1.4 \times 10^{15} (A_V - 1.0)$	$0.7 \times 10^{14} (A_V - 1.9)$	$2 < A_V < 4$	18
Taurus		$2.4 \times 10^{14} (A_V - 2.9)$	$5 < A_V < 11$	18
ρ Oph	$2.7 \times 10^{15} (A_V - 1.6)$	$1.7 \times 10^{14} (A_V - 3.9)$		18
Heiles # 2	$1.3 \times 10^{15} (A_V - 0.5)$	$2.5 \times 10^{14} (A_V - 1.5)$		19
L1495	$2.0 \times 10^{15} (A_V - 0.5)$	$2.2 \times 10^{14} (A_V - 1.1)$		20
Perseus	$2.5 \times 10^{15} (A_V - 0.8)$			11
L1506	$1.4 \times 10^{15} (A_V - 0.6)$			21
L1529	$0.9 \times 10^{15} (A_V - 0.9)$			21

measurements of CO column density versus visual extinction have generally been limited to visual extinctions less than 8 mag.

3. The ratio of CO to ^{13}CO is not well known and may be variable. In cold clouds ($T < 20$ K) the abundance of ^{13}CO is enhanced by chemical fractionation. That is, it is energetically more favorable to form ^{13}CO than CO ($\Delta E/k \approx 35$ K), so that an atom of ^{13}C will preferentially exchange with ^{12}C in CO. In cold clouds there is not enough kinetic energy available to reverse the exchange and the abundance of ^{13}CO will eventually be enhanced.[12]
4. On the edges of clouds ^{13}CO and $C^{18}O$ are selectively photodissociated because their abundances are not high enough for self-shielding from the ambient interstellar radiation field. Thus at low extinctions, the column density derived from these species underestimates the total abundance of CO.[13]

C I ABUNDANCES

Since we have established the CO to H_2 relation, it is now only necessary to compare CI and CO directly.[22,23,24] Again the LTE method of abundance calculation is discussed in the Appendix. Unfortunately, the collisional excitation of C I by H_2 is not well understood. A recent estimate gives $\sim 10^4$ cm^{-3} for the critical density of the $^3P_1 \rightarrow {}^3P_0$ transition.[25] If the new estimate is correct the validity of the LTE method of abundance determination is questionable. Earlier estimates were ~ 2000 cm^{-3}, approximately the same as ^{13}CO.[26]

RESULTS FROM C I

In many cases it has been found that the spectral lines of the $^3P_1 \rightarrow {}^3P_0$ transition of C I strongly resemble the $J = 1 \rightarrow 0$ lines of ^{13}CO (e.g., see Figure 5), particularly the observed linewidths and lineshapes. The line intensities are also often similar. This implies that the optical depth of the C I lines is moderate and is similar to that of ^{13}CO and that the C I and ^{13}CO emission lines arise in areas of similar density and temperature.

Comparing Equations (9) and (11) in the Appendix we see that in a region in LTE with $T_{ex} = 30$ K having lines of C I and ^{13}CO of equal integrated intensity and optical depth the ratio $N(C\,I)/N(^{13}CO) = 7.5$. Since $N(CO)/N(^{13}CO) \approx 60$ in the Solar neighborhood that would imply that $N(C\,I)/N(CO) \approx 0.13$ or that about 3% of the total carbon abundance is in the form of C I in molecular clouds.

Figures 6 and 7 show that the situation is somewhat more complex than outlined above. These figures combine submillimeter and millimeter wavelength observations of C I and CO in the dense cloud associated with the star

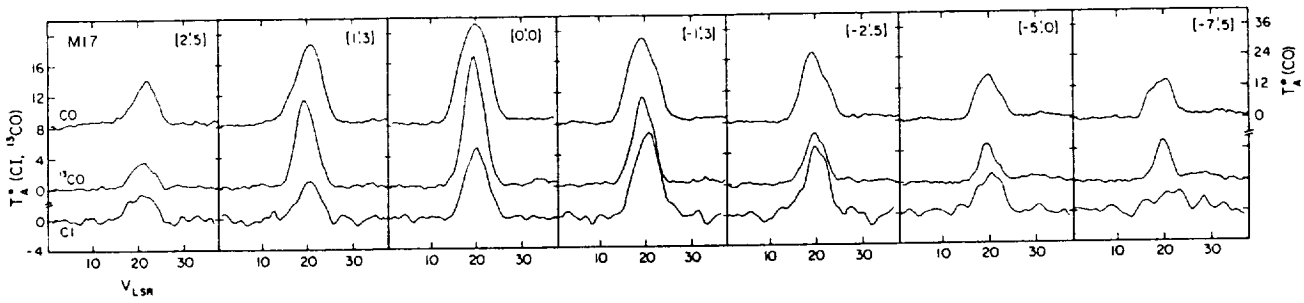

FIG. 5. – A comparison of the lines of CO, ^{13}CO and C I across the ionization front in M17.[23] The ionization front is at position 2'.5 and the dense molecular cloud lies to the right. The intensity scale of the CO line is a factor of 3 smaller than the C I and ^{13}CO scales in the plot. The C I line bears a strong resemblance to the ^{13}CO line at most of these positions.

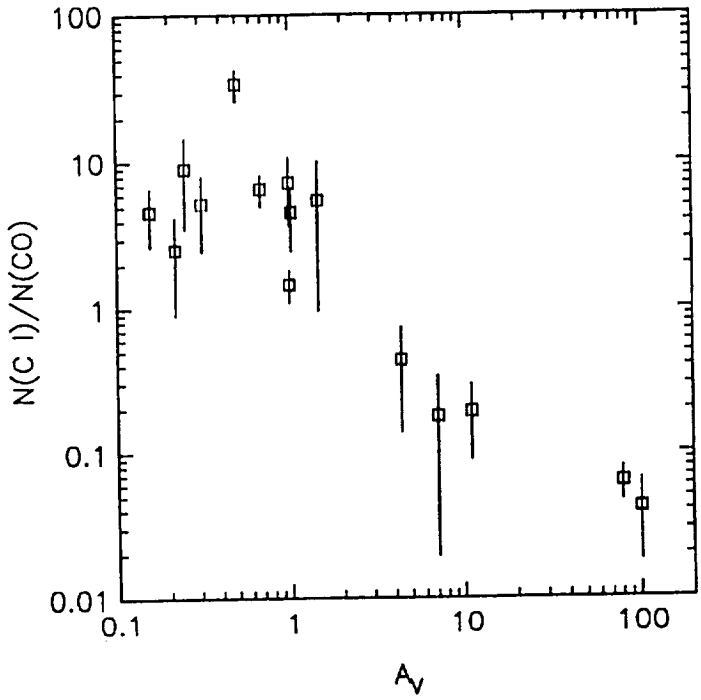

FIG. 6. – The ratio of N(C I) to N(CO) as a function of A_V. In diffuse clouds the ratio generally has values of 2–10; within moderately opaque dense clouds, $4 < A_V < 30$ mag, the ratio decreases from about 0.5 to 0.1; at higher A_V's the ratio appears to drop further but this effect may be due to strong self-absorption in the C I line. At $A_V < 2$ the data are from ultraviolet absorption observations,[27,28] at higher A_V's they are from millimeter and submillimeter emission line observations.[24]

ρ Ophiuchi with ultraviolet observations of C I and CO in diffuse clouds.[24,27,28] It can be seen in Figure 6 that the ratio N(C I)/N(CO) decreases from about 5 to 0.1 as the extinction increases from A_V of about 1 to 30. At higher A_V's the ratio appears to decrease further but, as discussed in the next section, that conclusion is confused by the high opacity and resultant self-absorption of the C I lines at large A_V.

Figure 7 shows the results of comparing N(C I) with N(H+2H$_2$). The interesting points are that the fractional abundance of C I is low outside dense clouds ($A_V < 1$), is fairly constant within dense clouds ($4 < A_V < 30$) at 10^{-5} relative to hydrogen, i.e. 3% of the total abundance of carbon, and may decrease in the centers of dense clouds ($A_V > 30$), but the behavior at the largest extinctions is not yet well established.

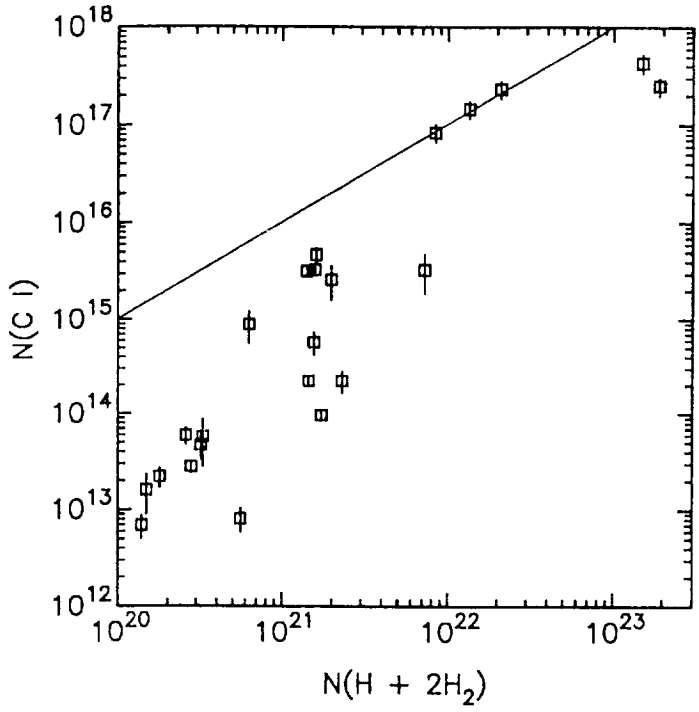

FIG. 7. – The column density of C I as a function of total hydrogen column density. The line indicates a constant $N(\mathrm{C\,I}) / N(\mathrm{H}+2\mathrm{H_2})$ ratio of 10^{-5} or 3% of the cosmic abundance of carbon in the form of C I. The data for $N(\mathrm{CI}) < 10^{16}$ are from ultraviolet observations of diffuse clouds[27] and for higher values from submillimeter observations of the dense dark cloud associated with ρ Ophiuchi. It can be seen that the fractional abundance of CI reaches a peak in moderately opaque clouds, $8\times10^{21} < N(\mathrm{H}+2\mathrm{H_2}) < 4\times10^{22}$ or $4 < A_V < 20$. It may decrease at higher opacities but that conclusion is as yet uncertain.

Figures 5–7 show that the simple picture of C I distribution developed by the classical photodissociation models (Fig. 1) does not match the observations. The abundance of C I is higher throughout molecular clouds than is predicted by such models. The generally high abundances observed via the $^3P_1 \rightarrow {}^3P_0$ line have been confirmed recently by observations of the $^3P_2 \rightarrow {}^3P_1$ line.[29,30] Many models have been produced to explain these observations (see the review by Keene *et al.*[23]). An attractive model has been proposed in connection with C I and C II line observations of M17.[29] In this model the molecular cloud is assumed to be clumpy, allowing ultraviolet radiation from exterior and interior sources to reach most parts of the molecular cloud, producing C I (and C II) throughout the cloud.

PROBLEMS WITH C I ABUNDANCE DETERMINATIONS

The problems associated with determining the abundance of C I are similar to those associated with CO.

1. The excitation temperature is unknown and is often assumed to be same as the CO excitation temperature. Knowledge of the temperature is necessary to calculate the partition function, correcting for the population in unobserved energy levels. The level populations depend on the critical density for excitation by H_2 which has not yet been calculated.
2. The optical depth of the C I lines is also unknown. The lines usually appear to be of moderate optical depth so opacity corrections are not unreasonably large. However, at large extinctions, the C I lines are seen to be optically thick and occasionally display symptoms of self-absorption similar to that often seen in CO and, less commonly, in ^{13}CO. Figure 8 contains an example of a high-extinction region in the ρ Oph dark cloud which has both strong CO and ^{13}CO self-absorption. This is evident in the high degree of asymmetry of the lines and the displacement of their peak velocities relative to the more optically thin C^{18}O. It is clear

from Figure 8 that C I also shows effects of self-absorption. Unfortunately, measuring the optical depth of the C I transitions, independent of CO observations, is difficult. It is not possible to observe the $^3P_1 \rightarrow {}^3P_0$ transition of ^{13}C I because the brightest hyperfine component is separated from the C I line by only about 3 MHz (1.8 km s^{-1}), less than the linewidth in a typical warm cloud. Although it should be possible to observe the $^3P_2 \rightarrow {}^3P_1$ transition of ^{13}C I – the $F = 5/2 \rightarrow 3/2$ hyperfine component of the ^{13}C I $^3P_2 \rightarrow {}^3P_1$ line is separated from the C I line by about 153 MHz (57 km s^{-1})[31] – it has not yet been done. Since the optical depths are often only moderate in both the C I lines the corresponding ^{13}C I lines will be difficult to detect.

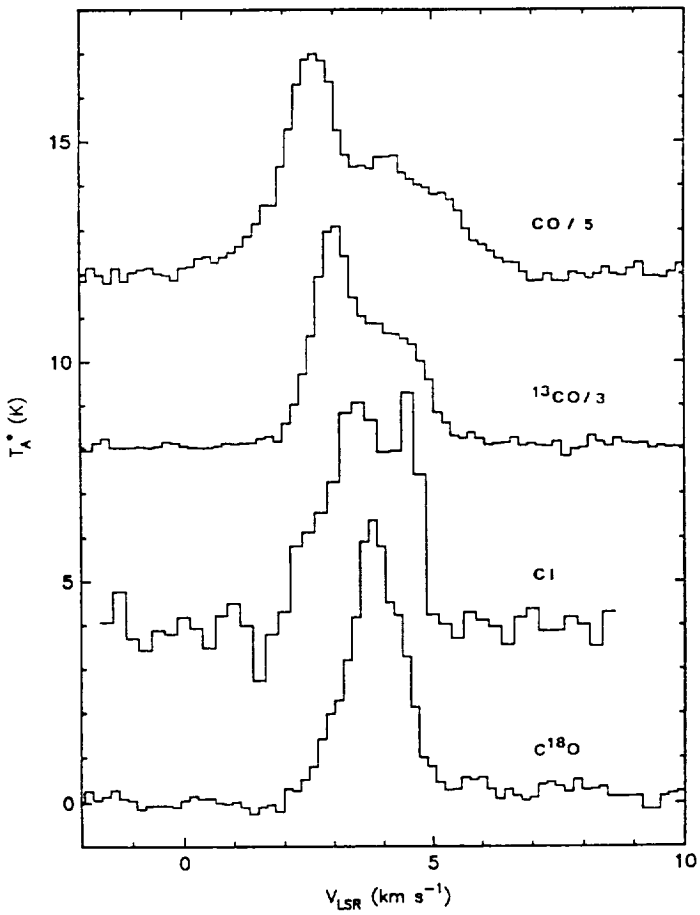

FIG. 8. – A comparison of the spectral lines of CO and its rarer isotopes with C I in the ρ Oph dark cloud.

OPPORTUNITIES FOR FUTURE WORK ON C I

Although there remain problems with the C I observations and unanswered questions about the abundance of C I, the hopes for future work are high. Submillimeter emission from the $^3P_1 \rightarrow {}^3P_0$ transition of C I was first observed in 1979 and the $^3P_2 \rightarrow {}^3P_1$ transition was first observed in 1985.[32,33] There has not yet been a systematic program to observe both of these transitions at the same positions with the same angular resolutions. When this is done the results should place constraints on the temperature and optical depths of the regions. Also, the earth's atmosphere is partially transparent (from very dry sites) at the wavelengths of both the $^3P_1 \rightarrow {}^3P_0$ and $^3P_2 \rightarrow {}^3P_1$ transitions. This means that the new submillimeter wavelength telescopes which are just being commissioned at the Mauna Kea Observatory and other places will be useful for making such studies of C I.

High spatial resolution observations will enable us to study the detailed distribution of C I, and to determine whether it has a smooth or clumpy distribution. If there are strong localized abundance peaks we will have to interpret them as being caused by localized sources of C I, such as embedded stars or nearby H II regions. It is also important to determine whether the C I fractional abundance decreases at the densest positions in molecular cloud cores or whether that apparent effect is an artifact of high opacity in the C I $^3P_1 \rightarrow {}^3P_0$ line.

C II ABUNDANCES

The $^2P_{3/2} \rightarrow {}^2P_{1/2}$ transition of C II lies in an opaque region of the atmosphere and can only be observed from above most of the earth's atmospheric water vapor, i.e., from an airplane, balloon, or spacecraft. This limits the spatial resolution with which it can be observed and the length of time spent observing it. Also until very recently it had been observed only at low spectral resolution with either grating or Fabry-Perot spectrometers.[34,35] Even with the relatively low resolution available ($200 < \nu/\Delta\nu < 1.2 \times 10^4$; $1500 > \Delta V > 25$ km s^{-1}) it was obvious that C II emission is related to CO $J = 1 \rightarrow 0$ emission.

RESULTS FROM C II

The distribution of C II emission across the Galactic plane resembles that of CO, not in detail but enough to see that it is closely associated with molecular clouds.[36] Also, over two orders of magnitude and in many different objects, the C II line intensity has been observed to be proportional to the intensity of the $J = 1 \rightarrow 0$ line of CO (Figure 9).[35] These observations similarly imply that the C II emission is intimately associated with molecular clouds. Since the presence of C II emission necessarily indicates that ultraviolet radiation is present, these results have been interpreted in terms of warm, $T \approx 300$ K, photodissociation regions lying at the interfaces between bright H II regions and molecular clouds.[4,35] At such a high temperature the emission from such regions would be optically thin.

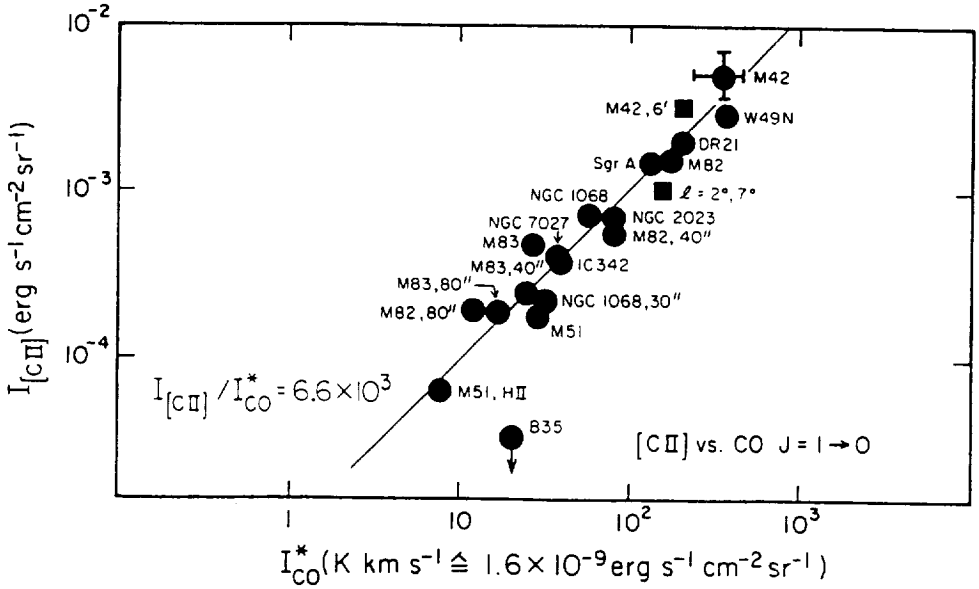

FIG. 9. – Correlation between C II and CO integrated line intensities for Galactic molecular clouds and other galaxies.[35]

Extensive observations of C II in the M17 region have shown that the emission is spread widely through the entire cloud, not just concentrated at the H II region, molecular cloud interface.[37] In fact the C II line intensity away from the interface follows the CO intensity and is a factor of 20 higher than predicted by photodissociation models. This has been interpreted as being due to a possible clumpy structure of the M17 molecular cloud which

allows ultraviolet radiation from *a*) luminous, hot, young stars within the H II region, *b*) less luminous and hot stars embedded within the molecular cloud, and *c*) the general interstellar radiation field to penetrate the entire molecular cloud, producing C II (and also C I) throughout the cloud.

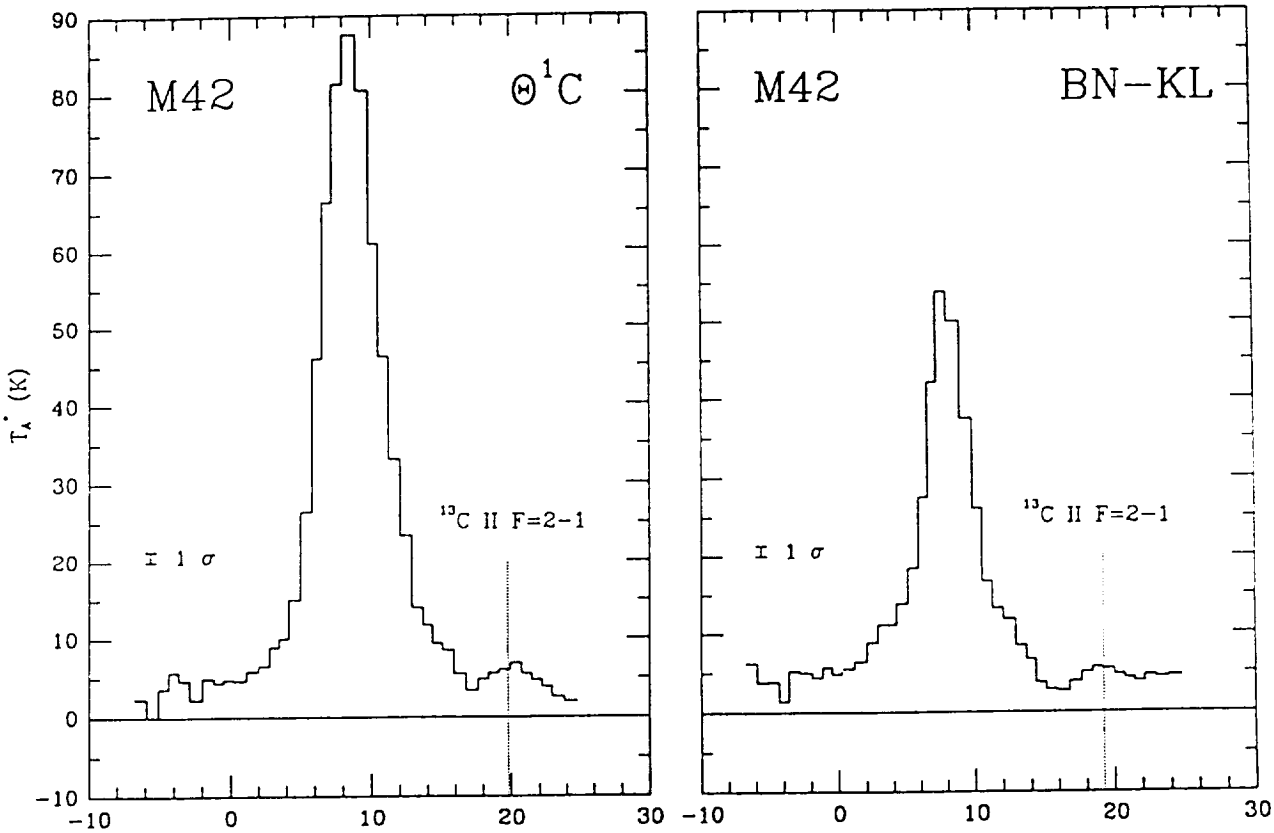

FIG. 10. – Spectra of the $^2P_{3/2} \rightarrow {}^2P_{1/2}$ line of C II from two positions in the Orion Nebula.[38]

Recent heterodyne observations have modified the above interpretations somewhat. Figure 10 shows the results of observations of C II at two positions in the Orion Nebula.[38] The main line in each spectrum, of course, is that of C II; about 11 km s^{-1} toward higher velocity is a feature which possibly is the $F = 2 \rightarrow 1$ hyperfine line of ^{13}C II. If the feature is real it implies that the optical depth in the main line is high, $\tau \approx 5$. In addition, since the optical depth is probably large and the critical density of C II is small (10^3 cm^{-3}), the observed brightness temperature is equal to the excitation temperature unless there is a non-unity beam filling factor. In OMC-1 the Planck corrected brightness temperature is in the range 90–130 K, thus the emission originates from regions closer to 100 K than 300 K in temperature, similar to the temperature in the molecular region.

It is difficult, without the benefit of large Galactic surveys, to calculate the total amount of C II. We can nevertheless get some idea of the amount of C II from surveys of many objects. Assuming that the C II emission is optically thin and originates in high temperature regions where all the carbon is in the form of C II, Crawford *et al.*[35] have calculated that the ratio of mass in C II regions to that in molecular clouds, H_2 regions, is at least 3%. The heterodyne spectroscopy by Boreiko, Betz, and Zmuidzinas[38] show that this estimate may be low by a factor of as much as 5 (cf. eq. [14] in the Appendix). Therefore probably about 5–15%, say 10%, of the Galactic carbon associated with molecular clouds may be found in the form of C II.

PROBLEMS WITH AND OPPORTUNITIES FOR C II ABUNDANCE DETERMINATIONS

Because the excitation energy of the $^2P_{3/2}$ level is high it is difficult to observe in cold regions. Thus the estimate given above, 10% of Galactic carbon in molecular clouds in the form of C II, really only refers to high-

temperature regions associated with star formation where the levels of ultraviolet radiation are enhanced. We have not yet measured the possibly much lower abundance of C II associated with dark molecular clouds.

As is the case with C I, the determinations of the kinetic temperature of emission regions and line optical depths present problems for the interpretation of C II observations. Luckily, with the advent of sensitive far-infrared heterodyne spectrometers that problem is ripe for solving. The $^2P_{3/2} \rightarrow {}^2P_{1/2}$ line of C II is considerably brighter than either the $^3P_1 \rightarrow {}^3P_0$ or $^3P_2 \rightarrow {}^3P_1$ line of C I so that observations of the $F = 2 \rightarrow 1$ hyperfine component of the ^{13}C II $^2P_{3/2} \rightarrow {}^2P_{1/2}$ line are possible. Measurement of the brightness of that line in many sources will lead to a better determination of the overall C II abundance.

Also with the high sensitivity and frequency resolution of heterodyne receivers now available we can begin to develop an understanding of the relative kinematics of the C II and various atomic and molecular components of the dense gas.

SUMMARY

In the dense interstellar medium, we find that about 20% of the total carbon abundance is in the form of CO, about 3% in C I, and 10% in C II with uncertainties of factors of order 2. The abundance of other forms of gaseous carbon is negligible. CO is widespread throughout molecular clouds as is C I. C II has only been observed near bright star-formation regions so far because of its high excitation energy. Further from ultraviolet sources it may be less abundant. Altogether we have accounted for about 1/3 of the total carbon abundance associated with dense molecular clouds. Since the other gaseous forms are thought to have negligible abundances the rest of the carbon is probably in solid form.

APPENDIX

CO Column Densities

CO is an example of the most common type of diatomic molecule, in its ground electronic state it has no net electronic angular momentum, i.e., the ground electronic state is $^1\Sigma$. This greatly decreases the number of available energy levels and facilitates the calculation of their energies and transition probabilities. The rotational states in the ground vibrational state (displayed for CO in Figure 3) have energies above the $J = 0$ ground state which are given to first order by $E_J = J(J+1)hB$, where $J = 0, 1, 2...$ is the rotational quantum number (actually the total angular momentum quantum number) and B is the rotational constant. For CO, $hB/k = 2.77$ K, for ^{13}CO, 2.64 K and, for C^{18}O, 2.63 K. The statistical weights of the levels are given by $g_J = 2J + 1$.

If the emission lines under consideration are optically thin, which is almost certainly the case for ^{13}C^{18}O and C^{17}O, is often the case for C^{18}O, is sometimes the case for ^{13}CO, and is almost never the case for CO, the calculation of column densities is relatively straightforward. The average column density of molecules in the telescope beam in upper level J, N_J, is simply related to the energy intensity averaged over the telescope beam, $\bar{I}_\nu$, as

$$N_J = \frac{4\pi}{A_{J,J'} h\nu} \int \bar{I}_\nu \, d\nu. \tag{1}$$

$A_{J,J'}$ is the Einstein coefficient for spontaneous emission in the $J \rightarrow J'$ transition.

In millimeter-wave astronomy the energy intensity is more conveniently expressed in temperature units proportional to the average energy intensity in the beam. The "antenna temperature" corrected for all telescope losses, T_A^* also sometimes called T_R^*, is such a unit. Its definition is

$$\frac{kT_A^*}{h\nu} = \frac{c^2 \bar{I}_\nu}{2h\nu^3}. \tag{2}$$

In the long-wavelength or high-temperature limit, T_A^* is the temperature of a blackbody with intensity $\bar{I}_\nu$, but in the submillimeter and far-infrared wavelength regions the Planck corrections are usually not negligible.

In terms of the observed antenna temperature, the average column density of molecules in state J observed via the optically thin $J \rightarrow J'$ emission line is

$$N_J = \frac{8\pi k\nu^2}{A_{J,J'}hc^3} \int T_A^* \, dV, \tag{3}$$

where the integral is taken over all velocities in the line.

The Einstein A coefficient for any transition is related to the dipole matrix element, $\mid \mu_{J',J} \mid$, by

$$A_{J,J'} = \frac{64\pi^4}{3h} \frac{\nu^3}{c^3} \frac{g_{J'}}{g_J} \mid \mu_{J',J} \mid^2 . \tag{4}$$

For a molecule with a $^1\Sigma$ electronic ground state, the dipole matrix element is given by

$$\mid \mu_{J-1,J} \mid^2 = \mu^2 \frac{J}{2J-1} \tag{5}$$

and radiative transitions other than $\Delta J = \pm 1$ are forbidden. The dipole moment, μ, for CO (as well as all its isotopes) is 0.11 Debyes (0.11×10^{-18} cgs), thus the Einstein $A_{1,0}$ coefficient for CO is 7.2×10^{-8} s^{-1}, for ^{13}CO is 6.3×10^{-8} s^{-1}, and for C^{18}O is 6.2×10^{-8} s^{-1}.

To calculate the total abundance of molecules we must correct for those in levels other than the observed one. The distribution of molecules among the various levels is commonly parameterized by the "excitation temperature", T_{ex}. The ratio of the population in level J, n_J, to that in the level J', $n_{J'}$, is given by the Boltzmann equation,

$$\frac{n_J}{n_{J'}} = \frac{g_J}{g_{J'}} \exp\left(-\frac{E_J - E_{J'}}{kT_{ex}}\right), \tag{6}$$

which is actually the definition of excitation temperature. The "partition function" is the function that is needed to correct the abundance calculation in equation (1) to the total abundance. For a molecule with only angular momentum states J available the partition function, f, is

$$f = \sum_J g_J \exp(-E_J/kT_{ex}). \tag{7}$$

A good approximation to this function (for a $^1\Sigma$ electronic ground state molecule at high T_{ex}) is $f = kT_{ex}/hB$.[39]

The expression for the partition function given above has made use of a very common approximation, i.e., that all the CO energy levels are characterized by the same excitation temperature which is the local gas kinetic temperature. This approximation is described by the term "local thermodynamic equilibrium" (LTE). The kinetic temperature of isothermal gas in LTE is equal to the brightness temperature of an optically thick emission line, in this case the CO $J = 1 \rightarrow 0$ emission line. This LTE assumption is approximately valid for the following reason.

At densities higher than the "critical density" for a given molecular transition, the excitation temperature approaches the kinetic temperature of the gas. In the limit of zero optical depth the critical density is the space density at which the rate of collisional de-excitations of a given energy level is equal to the rate of radiative de-excitations. However, if the emission lines resulting from radiative de-excitation are optically thick then the critical density is decreased by a factor of about τ, the optical depth.[40] In dense clouds, low-lying transitions of CO are optically thick and easily excited – the critical density of the $J = 1 \rightarrow 0$ transition is $n(H_2) \approx 2500$ cm^{-3}. Since τ(CO) is typically 50 to 100, it is obvious that these low energy states of CO should be thermalized, i.e., in LTE, in dense clouds. It is less clear that the states of the rare CO isotopic species will be in LTE. The assumption of LTE for these species is likely to overestimate their abundance since the upper energy levels are probably underpopulated relative to their lower ones.

The total number of molecules is related to the integrated antenna temperature of an optically thin line as

$$N_T \approx \frac{1}{g_J} \exp\left(\frac{E_J}{kT_{ex}}\right) f \frac{8\pi k\nu^2}{A_{J,J'}hc^3} \int T_A^* \, dV. \tag{8}$$

If the line used in the above analysis has moderate optical depth, i.e., $\tau \sim 1$, we can multiply the result by $\tau_o/(1 - e^{-\tau_o})$, where τ_o is the optical depth at the center of the line, as an approximate correction. The central optical depth can be derived from comparison of the line brightness with the brightness in an optically thick line, i.e., CO $J = 1 \rightarrow 0$.

For the $J = 1 \rightarrow 0$ line of both ^{13}CO and $C^{18}O$ the final result for the total isotopic abundance is

$$N_T \approx 4.7 \times 10^{13}\, T_{ex} \exp\left(\frac{5.3}{T_{ex}}\right) \frac{\tau_o}{(1 - e^{-\tau_o})} \int T_A^* \, dV, \tag{9}$$

where $\int T_A^* \, dV$ is measured in units of K km s^{-1}.

Finally the abundance must be corrected to the main isotope by using the isotopic abundance ratios. These are typically taken to be $N(CO)/N(^{13}CO) \approx 60$ and $N(CO)/N(C^{18}O) \approx 500$.[7]

C I Column Densities

We analyze the C I column density as we did that of CO, making use of the same definitions for excitation temperature and partition function. The carbon atom has a ^3P ground term, split by spin-orbit coupling into three levels. The total electronic angular momentum quantum number, called J, has the values 0, 1 and 2 resulting in ground term levels $^3P_0$, $^3P_1$ and $^3P_2$. The statistical weights, g_J, of these lowest three energy levels are again equal to $2J + 1$.

Because C I has only three accessible energy states at temperatures common in the interstellar medium ($T < 100$ K), with energies $E_0 = 0$, $E_1/k = 23.6$ K and $E_2/k = 62.5$ K, the partition function is given by

$$f = 1 + 3\exp\left(-\frac{23.6}{T_{ex}}\right) + 5\exp\left(-\frac{62.5}{T_{ex}}\right). \tag{10}$$

The total number of atoms of atomic carbon observed in an optically thin line is given by equation (8). The Einstein $A_{1,0}$ coefficients for C I are $A_{1,0} = 7.9 \times 10^{-8}$ s^{-1} and $A_{2,1} = 2.7 \times 10^{-7}$ s^{-1}.[41] Inserting the numerical constants for the $^3P_1 \rightarrow {}^3P_0$ line of C I in equation (8) and including the correction for finite optical depth, we obtain for the total number of C I atoms

$$N_T = 1.9 \times 10^{15} \left[\exp\left(\frac{23.6}{T_{ex}}\right) + 3 + 5\exp\left(-\frac{38.0}{T_{ex}}\right)\right] \frac{\tau_o}{(1 - e^{-\tau_o})} \int T_A^* \, dV, \tag{11}$$

where again $\int T_A^* \, dV$ is measured in K km s^{-1}.

The collisional cross sections for C I with H_2 have not been calculated, so the critical density for excitation of C I by H_2 is not well known. However, Monteiro and Flower[25] estimate that the cross section for excitation of the $^3P_1$ level from the $^3P_0$ level by H_2 is about 0.1 times the cross section for excitation by atomic hydrogen calculated by Launay and Roueff.[42] That makes the critical density for the $^3P_1 \rightarrow {}^3P_0$ transition $\sim 10^4$ cm^{-3}. With such a high critical density the LTE assumption may be questionable. Luckily the $^3P_2 \rightarrow {}^3P_1$ transition is observable and seems to have a smaller critical density for excitation by H_2 than does the $^3P_1 \rightarrow {}^3P_0$ transition.

C II Column Densities

Singly ionized carbon, C II, has a ^2P ground state term, split by spin-orbit coupling into the levels $^2P_{1/2}$ and $^2P_{3/2}$. Again, the statistical weight of each level is $2J+1$ where J has the values 1/2 and 3/2. The energies of the levels are $E_{1/2} = 0$ and $E_{3/2}/k = 91.2$ K. In the dense interstellar medium only these two levels have significant populations.

To solve for the number of ionized carbon atoms we once again assume that the population distribution of the C II energy levels can be described by LTE. The partition function is then

$$f = 2 + 4\exp\left(-\frac{91.2}{T_{ex}}\right). \tag{12}$$

The value of the Einstein A coefficient for the $^2P_{3/2} \rightarrow {}^2P_{1/2}$ transition is 2.4×10^{-6} s^{-1}. The total number of atoms of ionized carbon is

$$N_T \approx 1.5 \times 10^{15} \left[\exp\left(\frac{91.2}{T_{ex}}\right) + 2\right] \frac{\tau_o}{(1 - e^{-\tau_o})} \int T_A^* \, dV, \tag{13}$$

where the correction factor for finite optical depth has been included.

In the past it has not been common to express the intensity of C II emission in terms of antenna temperature because the lines are generally not spectrally resolved. In terms of energy intensity equation (13) can be written (as in eq. [1]),

$$N_T \approx 2.1 \times 10^{20} \left[\exp\left(\frac{91.2}{T_{ex}}\right) + 2\right] \frac{\tau_o}{(1 - e^{-\tau_o})} \int \bar{I}_\nu \, d\nu \tag{14}$$

where $\int \bar{I}_\nu \, d\nu$ is in units of ergs s^{-1} cm^{-2} sr^{-1}

REFERENCES

1. Kulkarni, S. R., and Heiles, C. 1987, in *Interstellar Processes*, eds D. Hollenbach and H. Thronson (Dordrecht: Reidel), p. 87.
2. Allen, C. W. 1973, *Astrophysical Quantities*, (London: Athlone Press).
3. Langer, W. D. 1976, *Ap. J.*, **206**, 699.
4. Tielens, A. G. G. M., and Hollenbach, D. 1985, *Ap. J.*, **291**, 722.
5. Leung, C. M., Herbst, E., and Heubner, W. F. 1984, *Ap. J. Supp.*, **56**, 231.
6. Audouze, J. 1977, in *CNO Isotopes in Astrophysics*, ed. J. Audouze (Dordrecht: Reidel), p. 3.
7. Wannier, P. G. 1980, *Ann. Rev. Astr. Ap.*, **18**, 399.
8. Bok, B. J., and Cordwell, C. S. 1973, in *Molecules in the Galactic Environment*, eds. M. Gordon and L. Snyder (Wiley-Interscience:New York), p. 53.
9. Dickman, R. 1978, *A. J.*, **83**, 363.
10. Bohlin, R. C., Savage, B. D., and Drake, J. F. 1978, *Ap. J.*, **224**, 132.
11. Bachiller, R., and Cernicharo, J. 1986, *Astr. Ap.*, **166**, 283.
12. Watson, W. D., Anicich, V. G., and Huntress, W. T. 1976, *Ap. J. (Letters)*, **205**, L165.
13. Bally, J., and Langer, W. D. 1982, *Ap. J.*, **255**, 143.
14. Encrenaz, P. J., Falgarone, E., Lucas, R. 1975, *Astr. Ap.*, **44**, 73.
15. Tucker, K. D., Dickman, R. L., Encrenaz, P. J., Kutner, M. L. 1976, *Ap. J.*, **210**, 679.
16. Dickman, R. 1978, *Ap. J. Supp.*, **37**, 407.
17. Elmegreen, D. M., and Elmegreen, B. G. 1979, *A. J.*, **84**, 615.
18. Frerking, M. A., Langer, W. D., and Wilson, R. W. 1982, *Ap. J.*, **262**, 590.
19. Cernicharo, J., and Guélin 1987, *Astr. Ap.*, **176**, 299.
20. Duvert, G., Cernicharo, J., Baudry, A. 1986, *Astr. Ap.*, **164**, 2.
21. Nercessian, E., Castets, A., Cernicharo, J., and Benayoun, J. J. 1988, *Astr. Ap.*, **189**, 207.
22. Phillips, T. G., and Huggins, P. J. 1981, *Ap. J.*, **251**, 533.
23. Keene, J., Blake, G. A., Phillips, T. G., Huggins, P. J., and Beichman, C. A. 1985, *Ap. J.*, **299**, 967.
24. Frerking, M. A., Keene, J., Blake, G. A., and Phillips, T. G. 1988, submitted to *Ap. J.*
25. Monteiro, T. S., and Flower, D. R. 1987, *M. N. R. A. S.*, **228**, 101.
26. Flower, D. R., Launay, J. M., and Roueff, E. 1978, in *Les Spectres des Molecules Simples au Laboratoire et en Astrophysique* (Liège: Université de Liège), p. 137.
27. Jenkins E. B., and Shaya, E. J. 1979, *Ap. J.*, **231**, 55.
28. Federman, S. R., Glassgold, A. E., Jenkins, E. B., and Shaya, E. J. 1980, *Ap. J.*, **242**, 545.
29. Genzel, R., Harris, A. I., Jaffe, D. T., and Stutzki, J. 1988, preprint.
30. Zmuidzinas, J., Betz, A. L., Boreiko, R. T., and Goldhaber, D. M. 1988, preprint.
31. Cooksy, A. L., Saykally, R. J., Brown, J. M., and Evenson, K. M. 1986, *Ap. J.*, **309**, 828.

32. Phillips, T. G., Huggins, P. J., Kuiper, T. B. H., and Miller, R. E. 1980, *Ap. J. (Letters)*, **238**, L103.
33. Jaffe, D. T., Harris, A. I., Silber, M., Genzel, R., and Betz, A. L. 1985, *Ap. J. (Letters)*, **285**, L59.
34. Russell, R., Melnick, G., Smyers, S. D., Kurtz, N. T., Gosnell, T. R., Harwit, M., and Werner, M. W. 1980, *Ap. J. (Letters)*, **250**, L35.
35. Crawford, M. K., Genzel, R., Townes, C. H., and Watson, D. M. 1985, *Ap. J.*, **291**, 755.
36. Stacey, G. J., Viscuso, P. J., Fuller, C. E., and Kurtz, N. T. 1985, *Ap. J.*, **289**, 803.
37. Stutzki, J., Stacey, G. J., Genzel, R., Harris, A. I., Jaffe, D. T., and Lugten, J. B. 1988, preprint.
38. Boreiko, R., Betz, A., and Zmuidzinas J. 1988, *Ap. J. (Letters)*, **325**, L47.
39. Goldreich, P., and Kwan, J. 1974, *Ap. J.*, **189**, 441.
40. White, R. E. 1977, *Ap. J.*, **211**, 744.
41. Nussbaumer, H. and Rusca, C., *Astr. Ap.*, **72**, 129.
42. Launay, J. M. and Roueff, E. 1977, *Astr. Ap.*, **56**, 289.